

Research Article

Comparative Antibacterial Study of Raw and C16TMA-Modified Kanemite for Environmental Water Disinfection

Fatima Zohra Sahli^{1*}, Mohamed Sassi², Abdallah Labbaci³

¹ Water and Environment Laboratory, Department of Processes Engineering, University of Hassiba Benbouali Chlef
* Corresponding Author Email: fatima191080@yahoo.fr - ORCID: 0000-0002-3305-5417

² Material Chemistry Laboratory - Department of Chemistry, University of Oran Ahmed ben bella, 3100 Oran, Algeria
Email: sassim2006@yahoo.fr - ORCID: 0000-0001-7488-4185

³ Water and Environment Laboratory, Department of Processes Engineering, University of Hassiba Benbouali Chlef
Email: ablabbaci@yahoo.fr - ORCID: 0000-0002-9198-1531

Article Info:

DOI: 10.22399/ijcesen.5193
Received : 30 September 2025
Revised : 05 April 2026
Accepted : 15 April 2026

Keywords

Antibacterial kinetics
Hexadecyltrimethylammonium
Intercalation
Kanemite;
Staphylococcus aureus
Water disinfection

Abstract:

Access to microbiologically safe water remains a critical public health challenge. Layered silicates like kanemite offer a platform for water disinfection, but their native form has limited antibacterial efficacy. This study comparatively evaluates raw kanemite and its organically modified form, cetyltrimethylammonium-kanemite (C16TMA-kanemite), to assess the impact of intercalation on antibacterial performance. Both materials were synthesized via a hydrothermal method and characterized using X-ray diffraction (XRD), Fourier-transform infrared spectroscopy (FTIR), and scanning electron microscopy (SEM). Antibacterial kinetics and minimum inhibitory concentration (MIC) against *Staphylococcus aureus* were monitored using UV-Vis spectrophotometry. Structural analysis revealed that while raw kanemite maintained a compact framework (d-spacing = 1.02 nm), the modified hybrid showed significant interlayer expansion to approximately 2.3–2.7 nm. Raw kanemite exhibited only partial inhibition at tested dosages, whereas C16TMA-kanemite achieved complete bacterial eradication (100%) within 15 minutes at 0.05 g/5 mL. These results demonstrate that organic modification is the decisive factor in transforming an inert silicate into a fast-acting biocide through membrane disruption, offering a potent solution for contaminated water disinfection.

1. Introduction

Access to microbiologically safe water remains one of the most critical public health challenges of the 21st century. According to recent reports by the World Health Organization [1], billions of people still lack access to safely managed drinking water services, exacerbating global health risks [2]. Waterborne pathogens, particularly *Staphylococcus aureus*, exhibit alarming persistence in urban and hospital wastewater effluents [3]. The continuous emergence of resistance genes in treated water now necessitates the use of more efficient nanotechnological strategies to combat multidrug-resistant strains [4,5]. In this context, the design of novel biocidal materials that are both efficient and economically viable has become a priority for

process engineering [6]. Synthetic layered silicates, specifically kanemite ($\text{NaHSi}_2\text{O}_5 \cdot 3\text{H}_2\text{O}$), are distinguished by their unique crystalline structure and exceptional surface reactivity. These minerals offer a versatile platform for molecular engineering due to their high ion-exchange capacity and the ease of tailoring their interlayer space [7,8]. However, native kanemite exhibits only limited antibacterial properties. To address this limitation, the intercalation of cationic surfactants, such as hexadecyltrimethylammonium bromide (C16TMA-Br), allows for the transformation of these inorganic matrices into hybrid organo-silicate nanocomposites with enhanced hydrophobic and biocidal properties [9,10]. These nanohybrids are now part of a sustainable chemistry approach for environmental safety [11]. The bactericidal

mechanism of these materials relies on a synergy between the silicate framework and the intercalated quaternary ammonium groups. The cationic heads interact electrostatically with the bacterial cell envelope, while the long hydrophobic alkyl chains penetrate and disrupt the lipid bilayer [12]. Recent studies have demonstrated that quaternary ammonium compounds significantly alter bacterial surface properties by reducing negative surface charge, disrupting membrane integrity, and inducing potassium leakage [13]. It has been confirmed that this insertion causes depolarization of the cytoplasmic membrane, leading to an irreversible leakage of intracellular constituents [10]. Although several studies have explored intercalated silicates, including the bactericidal activity of quaternary ammonium-modified silica powders against *Staphylococcus aureus* [14], systematic comparative kinetic data between raw kanemite and its organophilic form against Gram-positive bacteria remain scarce. In our previously published work [15], we reported the antibacterial activity of C16TMA-kanemite against *Staphylococcus aureus*. However, no data were available for pristine kanemite. In the present study, we provide for the first time: (1) the minimum inhibitory concentration (MIC) of pristine kanemite, and (2) a comparative kinetic analysis of both materials as a function of contact time. This study thus extends our previous work by providing the missing comparative data. The objective of the present work is to provide a detailed comparative study of the structural properties and antibacterial kinetics of kanemite and C16TMA-kanemite. Supported by rigorous characterization (XRD, FTIR, and SEM), we demonstrate how organic modification amplifies the bactericidal kinetics against *Staphylococcus aureus*, thereby opening new perspectives for advanced wastewater treatment.

2. Material and Methods

2.1. Chemical Reagents

Synthetic kanemite was used as the primary precursor. The organic modifier, hexadecyltrimethylammonium bromide (C16TMA-Br, $\geq 99\%$), was of analytical grade. Sodium silicate, sodium hydroxide (NaOH, $\geq 97\%$), and all other reagents were used as received without further purification. Deionized water was used throughout all synthesis and washing steps.

2.2. Synthesis and Organic Modification of Kanemite

The synthesis of kanemite was carried out following a hydrothermal route as originally described by Beneke and Lagaly [16]. Amorphous colloidal silica and sodium hydroxide were combined in a 1:1 molar ratio and dissolved in 100 mL of chilled methanol under continuous stirring. The resulting mixture was then dried in an oven at 100 °C for two weeks. The obtained solid was subsequently calcined at 700 °C for 5.5 hours. After gradual cooling to ambient temperature, the calcined product was dispersed in distilled water, filtered, washed, and finally air-dried at room temperature. The organic modification of kanemite was achieved via cation exchange at room temperature according to a protocol adapted from Kimura et al. [9, 17]. In a typical procedure, 1 g of kanemite was dispersed in 200 mL of an aqueous solution containing 0.1 M of hexadecyltrimethylammonium bromide (C16TMABr). The suspension was continuously stirred for 48 hours at room temperature to ensure complete ion exchange. The resulting organo-modified product (C16TMA-kanemite) was recovered by centrifugation, washed three times with distilled water to remove excess surfactant, and air-dried at room temperature.

2.3. Characterization Techniques

The crystalline structure of the synthesized materials was determined by powder X-ray diffraction (XRD) using Cu K α radiation ($\lambda = 0.1541$ nm) over a 2θ range of 2–40°. Functional groups were identified by Fourier-transform infrared (FTIR) spectroscopy in the range of 400–4000 cm $^{-1}$ using the KBr pellet technique. Surface morphology was examined by scanning electron microscopy (SEM) on gold-coated samples.

2.4. Antibacterial Activity Assessment

2.4.1. Minimum Inhibitory Concentration (MIC) Determination

The MIC of kanemite and C16TMA-kanemite was determined against *Staphylococcus aureus* (Gram-positive) using an agar incorporation method. Increasing masses of each material were separately mixed with 5 mL of molten nutrient agar in sterile tubes using a vortex mixer, then poured into sterile Petri dishes. After solidification, *S. aureus* was inoculated onto the surface of each plate. A control plate of non-supplemented nutrient agar was inoculated with the same strain. All plates were incubated at 37 °C for 24 h under aseptic conditions. The MIC was defined as the lowest

material mass at which no visible bacterial colony was observed [18].

2.4.2. Antibacterial Kinetics in Physiological Saline

To evaluate the antibacterial activity under aqueous conditions, kinetic experiments were carried out in physiological saline. A suspension of *Staphylococcus aureus* was prepared in 5 mL of physiological saline and adjusted to an optical density (OD_{600}) of 0.78, corresponding to approximately 10^8 CFU/mL, as measured with a UV-Vis spectrophotometer. An aliquot of 0.1 mL was withdrawn and transferred into a tube containing 10 mL of nutrient broth as the zero-time control ($t = 0$). The material mass corresponding to the MIC was then added to the bacterial suspension. The mixture was continuously agitated for 30 minutes; at each 5-minute interval, 0.1 mL was withdrawn via a sterile syringe and inoculated into a separate tube containing 10 mL of nutrient broth. All inoculated tubes were incubated at 37 °C for 24 h, after which the OD_{600} was measured for each tube. The procedure was performed independently for raw kanemite and C16TMA-kanemite [19].

3. Results and Discussions

3.1. XRD Structural Analysis

3.1.1. Kanemite

The XRD pattern of the synthesized kanemite (Fig.1) exhibits high crystallinity and displays the characteristic reflections of pure kanemite ($NaHSi_2O_5 \cdot 3H_2O$).

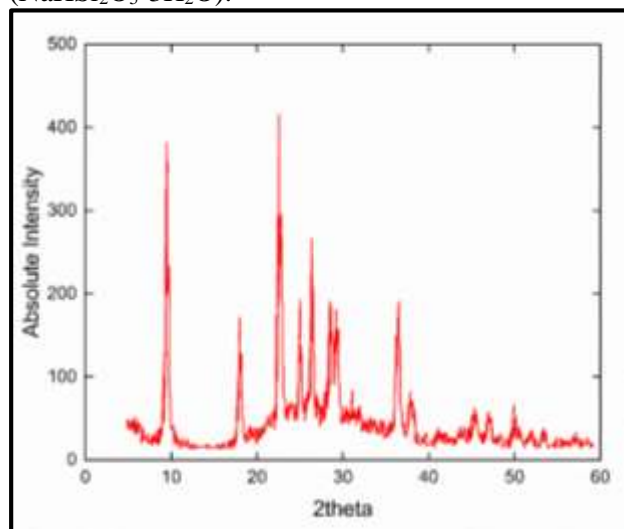


Figure 1. XRD pattern of the synthesized kanemite

The most intense peak at $2\theta = 8.65^\circ$ corresponds to the (001) basal reflection, yielding a d-spacing of approximately 1.02 nm. This value is in perfect

agreement with the literature for well-ordered layered silicates [16]. Additional sharp peaks at $2\theta \approx 21^\circ$, 24.5° , and 36° further confirm the formation of a stable, highly crystalline lamellar framework.

3.1.2. C16TMA-Kanemite

The XRD pattern of the C16TMA-kanemite nanocomposite (Fig.2) confirms the successful intercalation of the cetyltrimethylammonium cations into the silicate galleries. The original characteristic reflection at $2\theta = 8.65^\circ$ ($d = 1.02$ nm) has completely disappeared, replaced by a new intense basal reflection at a significantly lower angle ($2\theta \approx 3.2$ – 3.8°). According to Bragg's equation, the new interlayer distance has increased to approximately 2.3–2.7 nm. This expansion is a direct consequence of the bulky C16TMA⁺ chains adopting a paraffin-like monolayer or bilayer arrangement between the silicate sheets [9,20]. The broadening of the peaks in the hybrid material suggests a decrease in long-range crystalline order along the c-axis, typical of organo-silicates where organic chains introduce structural disorder [21,22]. This profound modification confirms the transition from a purely inorganic phase to a hybrid organo-silicate, creating a "contact-active" surface ready for antimicrobial application.

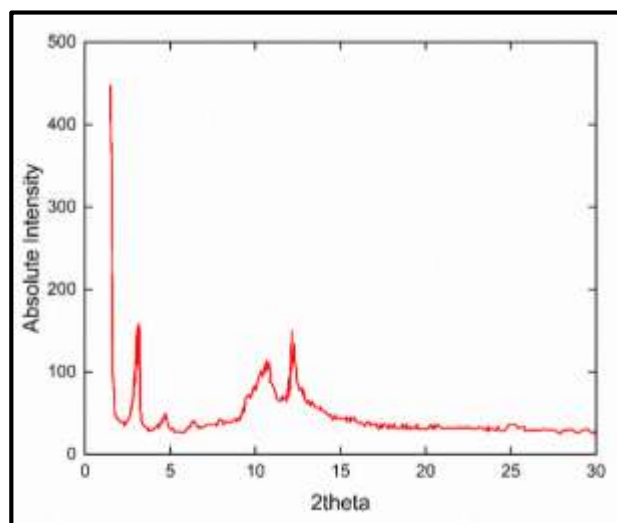


Figure 2. XRD pattern of the C16TMA-kanemite

3.2. FTIR Spectroscopic Analysis

The FTIR spectra of pristine kanemite (a), pure C16TMA⁺Br (b), and the C16TMA-kanemite hybrid (c) are compared in Fig.3.

The spectrum of pristine kanemite (a) displays characteristic bands at 3463 cm^{-1} and 3581 cm^{-1} , corresponding to the stretching vibrations of structural hydroxyl groups and interlamellar water molecules, consistent with the fundamental studies on layered silicates [23]. The bending vibration of

water is observed at 1630 cm^{-1} , while the intense peaks between 800 and 1150 cm^{-1} are attributed to Si–O–Si stretching of the silicate framework. For the C16TMA-kanemite hybrid (c), the success of the intercalation process is clearly evidenced by the emergence of new intense absorption bands at 2857 cm^{-1} (symmetric CH_2 stretch) and 2925 cm^{-1} (antisymmetric CH_2 stretch), while the deformation band at 1467 cm^{-1} confirms the presence of the cetyltrimethylammonium chains within the matrix [24]. The position of these CH_2 bands, both below 2926 cm^{-1} , indicates a predominantly ordered all-trans conformation of the alkyl chains, consistent with a densely packed bilayer arrangement [20]. The shift in the OH stretching region and the stability of the silicate backbone signals confirm that the organic cations have successfully replaced the interlayer hydrated sodium ions without compromising the structural integrity of the host

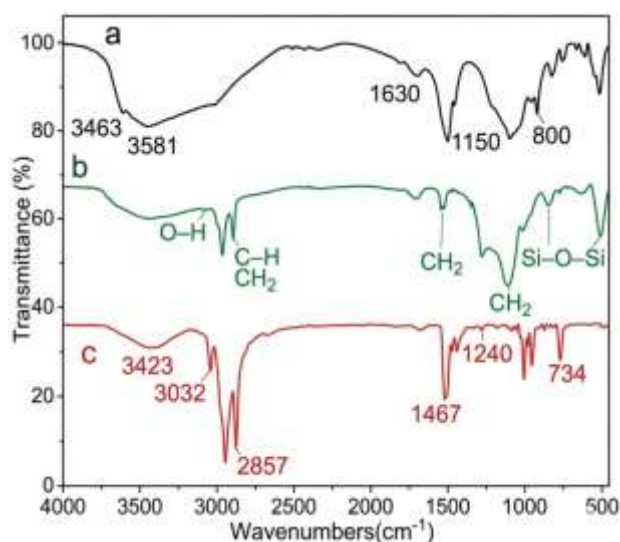


Figure 3. FTIR spectra of (a) kanemite, (b) C16TMABr, and (c) C16TMA-kanemite

3.3. Scanning Electron Microscopy (SEM) Analysis

SEM micrographs of both materials are shown in Figure 4. Pristine kanemite (Fig.4A) consists of well-defined plate-like crystallites assembled into dense aggregates, with lateral dimensions of $2\text{--}5\text{ }\mu\text{m}$, consistent with the high crystallinity evidenced by XRD [16,25]. The sharp edges and distinct layered appearance confirm the formation of a well-ordered lamellar phase. Upon organic modification with C16TMA (Fig.4B), the fundamental layered architecture is retained; however, the aggregates display a more "opened", partially delaminated appearance. This reorganization results from modification of inter-particle surface energy induced by the intercalated alkylammonium chains [25, 26]. , and is expected to increase the accessible

surface area for contact-killing activity against bacteria.

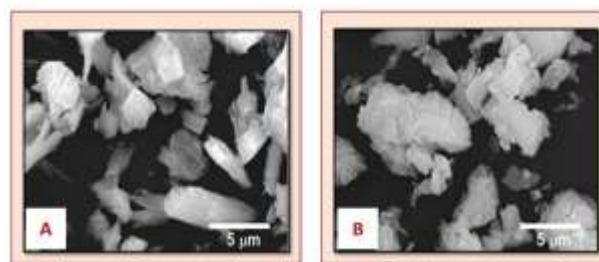


Figure 4. SEM micrographs of (A) raw kanemite and (B) C16TMA-kanemite.

3.4. Antibacterial Activity

3.4.1. Minimum Inhibitory Concentration (MIC)

The antimicrobial efficacy of the synthesized materials was evaluated against *Staphylococcus aureus* following a 24-hour incubation period. Representative agar plates are shown in Fig.5 and quantitative data are compiled in Table 1.

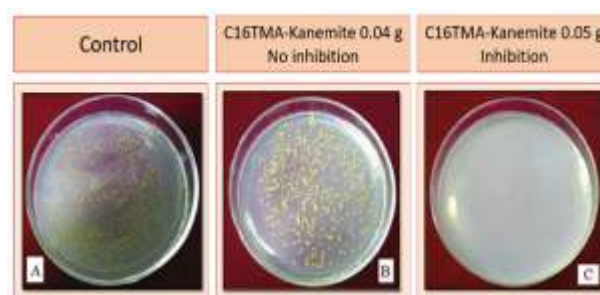


Figure 5. Antibacterial activity of C16TMA-kanemite against *S. aureus*

Table 1. MIC determination of kanemite against *Staphylococcus aureus*

Mass of kanemite (g)	10^{-3}	2.10^{-3}	3.10^{-3}
Inhibition	No inhibition	Inhibition	Inhibition

As shown in Fig.5 and Table 1, the C16TMA-kanemite hybrid exhibits a MIC of 0.05 g/5 mL against *S. aureus*. Raw kanemite shows only partial inhibitory effects (Table1), with no complete inhibition at any tested mass. The higher threshold required for the hybrid is attributable to the partial encapsulation of QA moieties within the silicate framework, which transiently limits their immediate bioavailability [27]. Nevertheless, once contact is established, the amphiphilic C16TMA⁺ groups exert a potent dual bactericidal action: (1) electrostatic attraction to the negatively charged components of the Gram-positive cell envelope (teichoic acids, peptidoglycan), followed by (2) insertion of the hydrophobic C16 alkyl chain into

the lipid bilayer, causing membrane perforation and irreversible cell lysis [28,29]. This dual mechanism transforms the silicate into a high-performance contact-active biocide.

3.4.2 .Comparative Antibacterial Kinetics

As demonstrated in Fig. 6, the kinetic profile of C16TMA-kanemite reveals an initial transient increase in optical density during the first 10 minutes of contact. This phenomenon is likely attributable to the rapid and massive release of intracellular constituents into the medium following the catastrophic disruption of the bacterial membranes [30]. Immediately after this peak, the optical density drops precipitously, reaching a baseline level by $t = 15$ min, signifying complete bacterial eradication. In sharp contrast, the raw kanemite profile exhibits only a gradual and incomplete reduction with notable fluctuations, consistent with a bacteriostatic rather than bactericidal mode of action [31,32]. This comparison confirms that organic functionalization with C16TMA⁺ transforms kanemite into a highly potent, rapid bactericidal material capable of total sterilization within 15 minutes, making it significantly more effective for antimicrobial water treatment applications.

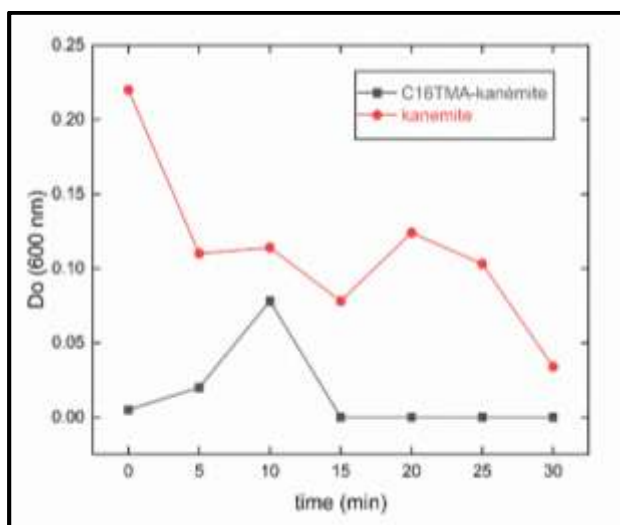


Figure 6. Comparative antibacterial kinetics of raw kanemite and C16TMA-kanemite against *S. aureus* as a function of contact time

C16TMA-kanemite shows a significant antibacterial effect against *Staphylococcus aureus*, reducing the optical density from 0.60 (control) to 0 within 15 minutes. This transformation from a passive silicate to a high-performance biocide is consistent with established strategies for the surface modification of layered silicates by quaternary ammonium for environmental applications [33]. These agents act by developing electrostatic

interactions between the cationic functional groups of the synthesized products and the negatively charged components of the bacterial outer wall [28,34]. This interaction disrupts the wall's function as a selective permeability barrier [12], leading to irreversible membrane damage and the subsequent leakage of intracellular constituents, which explains the transient peak observed in the kinetic profiles. In the case of pristine kanemite, the inhibitory effect observed during MIC determination can be attributed to its specific surface characteristics and high electron density [35]. However, in physiological saline, *S. aureus* demonstrated a capacity to bypass the antibacterial effect of raw kanemite. This resilience is often linked to chemotaxis mechanisms and the inherent resistance of Gram-positive strains to inorganic chemical environments [36].

4. Conclusions

This study successfully demonstrated the enhanced performance of C16TMA-kanemite compared to raw kanemite for the disinfection of water contaminated with *Staphylococcus aureus*. The synthesis of the layered polysilicate via the hydrothermal method was confirmed through rigorous characterization. The subsequent intercalation of the long-chain cationic surfactant C16TMA successfully expanded the interlayer spacing from 1.02 nm to 2.3–2.7 nm and generated a hybrid structure with high specific surface area, as validated by XRD and FTIR analysis. Biological assays revealed that the modified kanemite possesses a potent and rapid bactericidal effect, achieving complete bacterial inactivation within 15 minutes. This activity is fundamentally linked to the amphiphilic nature of the quaternary ammonium groups, which effectively disrupt and degrade the cytoplasmic membrane of Gram-positive bacteria. C16TMA-kanemite thus represents an efficient and promising material for water treatment applications. Future work should evaluate its efficacy against antibiotic-resistant strains and assess its performance in real wastewater matrices.

Author Statements:

- **Ethical Considerations:** This study does not contain any studies with human participants or animals performed by any of the authors. This research was conducted in compliance with standard laboratory biosafety and ethical guidelines.
- **Conflicts of Interest:** None declared.

- **Acknowledgments:** The authors would like to express their gratitude to the Water and Environment Laboratory at the University of Hassiba Benbouali, Chlef, and the Material Chemistry Laboratory at the University of Oran 1 Ahmed Ben Bella for providing the necessary facilities and support to conduct this research. Special thanks are also extended to the laboratory technicians for their technical assistance during the experimental phase.
- **Funding information:** The authors declare that this research was conducted as part of an academic study and did not receive any specific grant or financial support from funding agencies in the public, commercial, or not-for-profit sectors
- **Author contributions:** This work was accomplished through joint efforts.
- **Data availability statement :** The data that support the findings of this study are available from the corresponding author upon reasonable request.

References

- [1] World Health Organization & UNICEF. (2026). State of systems for drinking-water, sanitation and hygiene: global update 2025 (GLAAS 2025 report). World Health Organization. <https://www.who.int/publications/i/item/9789240118980>
- [2] Schwarzenbach, R. P., Egli, T., Hofstetter, T. B., von Gunten, U., & Wehrli, B. (2010). Global water pollution and human health. *Annual Review of Environment and Resources*. 35:109–136. <https://doi.org/10.1146/annurev-environ-100809-125342>
- [3] Endalamaw, K., Tadesse, S., Asmare, Z., Kebede, D., Erkihun, M., & Abera, B. (2024). Antimicrobial resistance profile of bacteria from hospital wastewater at two specialized hospitals in Bahir Dar city, Ethiopia. *BMC Microbiology*.24(1);525. <https://doi.org/10.1186/s12866-024-03693-8>
- [4] Mandal, T. K. (2024). Nanomaterial-enhanced hybrid disinfection: A solution to combat multidrug-resistant bacteria and antibiotic resistance genes in wastewater. *Nanomaterials*. 14(22);1847. <https://doi.org/10.3390/nano14221847>
- [5] Khoshmardan, M. E., et al. (2025). Unveiling the power of nanotechnology: A novel approach to eliminating antibiotic-resistant bacteria and genes from municipal effluent. *Environmental Geochemistry and Health*. 47(7);266. <https://doi.org/10.1007/s10653-025-02569-8>
- [6] Shannon, M. A., Bohn, P. W., Elimelech, M., Georgiadis, J. G., Marinas, B. J., & Mayes, A. M. (2008). Science and technology for water purification in the coming decades. *Nature*. 452(7185);301–310. <https://doi.org/10.1038/nature06599>
- [7] Saito, K., et al. (2024). Designed functions of oxide/hydroxide nanosheets via elemental replacement/doping. *Chemical Society Reviews*.53;10523–10574. <https://doi.org/10.1039/D4CS00339J>
- [8] Bergaya, F., & Lagaly, G. (2013). *Handbook of Clay Science* (Vol. 5). Elsevier.
- [9] Kimura, T., Itoh, D., Okazaki, N., Kaneda, M., Sakamoto, Y., Terasaki, O., Sugahara, Y., & Kuroda, K. (2000). Lamellar hexadecyltrimethylammonium silicates derived from kanemite. *Langmuir*.16(20);7624–7628. <https://doi.org/10.1021/la000325t>
- [10] Ioannou, C. J., Hanlon, G. W., & Denyer, S. P. (2007). Action of disinfectant quaternary ammonium compounds against *Staphylococcus aureus*. *Antimicrobial Agents and Chemotherapy*. 51(1);296–306. <https://doi.org/10.1128/AAC.00375-06>
- [11] Reda, A. T., & Park, Y. T. (2025). Sustainable synthesis of functional nanomaterials: Renewable resources, energy-efficient methods, environmental impact and circular economy approaches. *Chemical Engineering Journal*. 518;158573. <https://doi.org/10.1016/j.cej.2025.163894>.
- [12] Alkhalifa, S., Jennings, M. C., Granata, D., Klein, M., Wuest, W. M., Minbiole, K. P. C., & Carnevale, V. (2020). Analysis of the destabilization of bacterial membranes by quaternary ammonium compounds: A combined experimental and computational study. *ChemBioChem*. 21(10);1510–1516. <https://doi.org/10.1002/cbic.201900673>.
- [13] Nunes, B., Cagide, F., Borges, A., Borges, F., & Simoes, M. (2025). Antibacterial effects of novel quaternary ammonium and phosphonium salts against *Staphylococcus aureus*. *Journal of Applied Microbiology*. 136(6);lxaf122. <https://doi.org/10.1093/jambio/lxaf122>.
- [14] Suhara, T., Shimano, F., Sato, Y., Fukui, H., & Yamaguchi, M. (1996). Fine silica powder modified with quaternary ammonium group 4. Bactericidal activity. *Colloids and Surfaces A: Physicochemical and Engineering Aspects*.119;105–114. [https://doi.org/10.1016/s0927-7757\(96\)03762-4](https://doi.org/10.1016/s0927-7757(96)03762-4)
- [15] Sahli, F. Z., Sassi, M., Labbaci, A., & Laredj, H. (2018). Antibacterial effect of synthesized silicates for sewage treatment. *Biointerface Research in Applied Chemistry*. 8(2);3148–3152.
- [16] Beneke, K., & Lagaly, G. (1977). Kanemite—innercrystalline swelling and structural relations. *American Mineralogist*. 62(7–8);763–771.
- [17] Takahashi, N., Tamura, H., Mochizuki, D., Kimura, T., & Kuroda, K. (2007). Intercalation of poly(oxyethylene) alkyl ether into a layered silicate kanemite. *Langmuir*. 23(21);10765–10771. <https://doi.org/10.1021/la700974m>
- [18] Wiegand, I., Hilpert, K., & Hancock, R. E. (2008). Agar and broth dilution methods to determine the MIC of antimicrobial substances. *Nature Protocols*.

- 3(2);163–175.
<https://doi.org/10.1038/nprot.2007.521>.
- [19] Balouiri, M., Sadiki, M., & Ibsouda, S. K. (2016). Methods for in vitro evaluating antimicrobial activity: A review. *Journal of Pharmaceutical Analysis*. 6(2);71–79.
<https://doi.org/10.1016/j.jpha.2015.11.005>
- [20] Iwasaki, T., Wada, S., Nishitani, M., Okoshi, Y., & Horikoshi, H. (2025). Synthesis of kenyaite from synthetic silica glass scrap waste and organic modification using various quaternary alkylammonium salts. *Solid State Sciences*.160;107803.
<https://doi.org/10.1016/j.solidstatesciences.2024.107803>.
- [21] Vaia, R. A., & Giannelis, E. P. (1997). Lattice model of polymer melt intercalation in organically-modified layered silicates. *Macromolecules*.30(25);7990–7999.
<https://doi.org/10.1021/ma9514333>
- [22] Lagaly, G., Ogawa, M., & Dekany, I. (2013). Clay mineral organic interactions. In F. Bergaya & G. Lagaly (Eds.), *Handbook of Clay Science* (Vol.5,pp.435–505).Elsevier.
<https://doi.org/10.1016/b978-0-08-098258-8.00015-8>
- [23] Madejova, J. (2003). FTIR techniques in clay mineral studies. *Vibrational Spectroscopy*.31(1);1–10.
[https://doi.org/10.1016/S0924-2031\(02\)00065-6](https://doi.org/10.1016/S0924-2031(02)00065-6).
- [24] Vaia, R. A., Teukolsky, R. K., & Giannelis, E. P. (1994). Interlayer structure and molecular environment of alkylammonium layered silicates. *Chemistry of Materials*. 6(7);1017–1022.
<https://doi.org/10.1021/cm00043a025>.
- [25] Gilbert, P., & Moore, L. E. (2005). Cationic antiseptics: diversity of action under a common epithet. *Journal of Applied Microbiology*.99(4);703–715.
<https://doi.org/10.1111/j.13652672.2005.02664.x>.
- [26] He, H., Ma, L., Zhu, J., Frost, R. L., Theng, B. K. G., & Bergaya, F. (2014). Synthesis of organoclays: A critical review and some unresolved issues. *Applied Clay Science*. 100;22–28.
<https://doi.org/10.1016/j.clay.2014.02.008>.
- [27] Hazziza-Laskar, J., Helary, G., & Sauvet, G. (1995). Biocidal polymers active by contact. IV. Polyurethanes based on polysiloxanes with pendant primary alcohols and quaternary ammonium groups. *Journal of Applied Polymer Science*.58(1);77–84.
<https://doi.org/10.1002/app.1995.070580108>.
- [28] Lainioti, G. C., Druvari, D., & Kallitsis, J. K. (2024). Designing antibacterial-based quaternary ammonium coatings (surfaces) or films for biomedical applications: Recent advances. *International Journal of Molecular Sciences*.25(22);12264.
<https://doi.org/10.3390/ijms252212264>.
- [29] Zhang, J., Cheng, L., Li, H., et al. (2025). Challenges of quaternary ammonium antimicrobial agents: Mechanisms, resistance, persistence and impacts on the microecology. *Science of the Total Environment*. 958;178020.
<https://doi.org/10.1016/j.scitotenv.2024.178020>.
- [30] Benmamoun, Z., Chandar, P., Jankolovits, J., & Ducker, W. A. (2024). Time-resolved killing of individual bacterial cells by a polycationic antimicrobial polymer. *ACS Biomaterials Science & Engineering*. 10(5);3029–3040.
<https://doi.org/10.1021/acsbiomaterials.4c00263>
- [31] Co Lao, R. C., & Manglicmot Yabes, A. (2023). Time-kill kinetics of Piper betle L. ethanolic leaf extract on methicillin-sensitive *Staphylococcus aureus*. *Life Sciences, Medicine and Biomedicine*.7(1).
<https://doi.org/10.28916/lsm.7.1.2023.120>.
- [32] Yu, Z., Deng, C., Lei, T., et al. (2025). Cationic antibacterial polymers for development of bactericidal materials: Strategies, mechanisms, and applications. *Advances in Colloid and Interface Science*. 346;103658.
<https://doi.org/10.1016/j.cis.2025.103658>.
- [33] Sinha Ray, S., & Bousmina, M. (2005). Biodegradable polymers and their layered silicate nanocomposites: In greening the 21st century materials world. *Progress in Materials Science*.50(8);962–1079.
<https://doi.org/10.1016/j.pmatsci.2005.05.002>.
- [34] Munoz-Bonilla, A., & Fernandez-Garcia, M. (2018). Poly(ionic liquid)s as antimicrobial materials. *European Polymer Journal*. 105;135–149.
<https://doi.org/10.1016/j.eurpolymj.2018.05.027>
- [35] Vortmann, S., Rius, J., Marler, B., & Gies, H. (1999). Structure solution from powder data of the hydrous layer silicate kanemite, a precursor of the industrial ion exchanger SKS-6. *European Journal of Mineralogy*. 11(1);125–134.
<https://doi.org/10.1127/ejm/11/1/0125>
- [36] Schafer, D., Lam, T. T., Geiger, T., et al. (2009). A point mutation in the sensor histidine kinase SaeS of *Staphylococcus aureus* strain Newman alters the response to biocide exposure. *Journal of Bacteriology*. 191(23);7306–7314.
<https://doi.org/10.1128/JB.00630-09>.